Orbital ordering in $LaMnO_3$: Electron-electron and electron-lattice interactions

Satoshi Okamoto
The Institute of Physical and Chemical Research (RIKEN), Saitama 351-0198, Japan

Sumio Ishihara
Department of Applied Physics, University of Tokyo, Tokyo 113-8656, Japan

Sadamichi Maekawa
Institute for Materials Research, Tohoku University, Sendai 980-8577, Japan
(Received 24 October 2001; published 12 March 2002)

The interactions between e_g orbitals in neighboring sites are investigated in $LaMnO_3$ by taking into account virtual exchange of electrons and phonons. The spin and orbital ordering temperatures and the spin-wave dispersion relation are calculated. We find that the orbital ordering is mainly caused by the electronic interactions and that the Jahn-Teller coupling is much smaller than that reported previously. We propose that the elastic constant shows a characteristic change at the Néel temperature by the spin and orbital couplings and the higher-order Jahn-Teller coupling.

DOI: 10.1103/PhysRevB.65.144403 PACS number(s): 75.30.Et, 75.30.Vn, 71.10.−w, 62.20.Dc

I. INTRODUCTION

In some classes of transition-metal oxides, degeneracy of the *d* orbitals of a transition-metal ion remains and electrons have a degree of freedom indicating the occupied orbital. This is called the orbital degree of freedom.[1] For the colossal magnetoresistance (CMR) observed in perovskite manganese oxides,[2–4] the orbital degree of freedom is considered to play an important role, because the gigantic decrease of resistivity is observed in the vicinity of the transition from a charge and orbital ordered phase to a ferromagnetic metallic one. A parent compound of the CMR manganites, $LaMnO_3$, shows the orbital ordering below 780 K associated with the distortion of a MnO_6 octahedron. It has been experimentally confirmed that the orbital ordering is of *C* type[5] where two kinds of orbitals are alternately aligned in the *xy* plane and the planes are stacked along the *z* axis. In addition to the orbital ordering, the so-called *A*-type antiferromagnetic (AF) ordering appears below 145 K, where spins are aligned parallel (antiparallel) in the *xy* plane (*z* axis).[6,7] It is well recognized that this anisotropic magnetic ordering is stabilized by the orbital ordering.[5–15]

In $3d$ transition-metal compounds with orbital degeneracy, two kinds of mechanisms have been proposed for the orbital ordering. One is caused by the superexchange- (SE) type interaction between orbitals in different sites. This interaction originates from the virtual exchange of electrons under the strong on-site electron-electron interactions.[10,12] Another mechanism of the orbital ordering is based on cooperative Jahn-Teller (JT) effects where the lattice distortion occurs cooperatively and lifts the orbital degeneracy in the transition-metal ions.[16–19] The effective interaction between orbitals in this mechanism is caused by virtual exchange of phonons. However, it is usually difficult to separate contributions of these two mechanisms to the orbital ordering. This is because the two mechanisms provide the effective orbital interactions cooperatively.[20–23]

It has been supposed that the strong electron-lattice interaction that exists is necessary to explain CMR. The orbital ordering in $LaMnO_3$ was also studied based on the cooperative JT effects.[16,18,19] The energy splitting of the two e_g orbitals due to the lattice distortion termed the JT energy (E_{JT}) was estimated to be of the order of 1 eV by analyzing the orbital ordering temperature,[18] optical spectra,[24–29] and the energy-band calculation.[30–32] We note that in these analyses, the electron correlation effect was not taken into account properly. Actually, the on-site Coulomb interaction between electrons was estimated experimentally to be about 7 eV which is much larger than E_{JT}.[33] Therefore, it is necessary to reexamine the orbital ordering in $LaMnO_3$ by considering both the cooperative JT effect and the SE interaction under the strong electron correlation on an equal footing.

In this paper, we investigate the interactions between e_g orbitals in neighboring sites originating from the electron-electron and electron-lattice interactions in $LaMnO_3$. Magnitudes of these interactions are determined through the calculation of the spin and orbital ordering temperatures and the spin stiffness constants. It is shown that E_{JT} is much smaller than that in the literature[18,24–32] and the orbital ordering is mainly caused by the electronic interactions. We find that the elastic constant shows a characteristic change at the Néel temperature by which the coupling constant of the higher-order JT effect is estimated.

In Sec. II, the model Hamiltonian which describes the orbital interactions caused by exchanges of electrons and phonons is derived. In Sec. III, we introduce the mean-field approximation in the formulation of the orbital and spin ordering temperatures. In Sec. IV, by comparing the theoretical results of the ordering temperatures and the spin stiffness constants with the experimental values, the magnitudes of the orbital interactions are determined numerically. Temperature dependence of the elastic constants are studied in Sec. V. The last section is devoted to the summary and discussion.

II. MODEL

We start with the following Hamiltonian which includes spin, orbital, and lattice degrees of freedom:

$$\mathcal{H}=\mathcal{H}_e+\mathcal{H}_{e\text{-}latt}+\mathcal{H}_{latt}+\mathcal{H}_{str}+\mathcal{H}_{e\text{-}str}+\mathcal{H}_{hiJT}. \quad (1)$$

$\mathcal{H}_e$ describes the electronic interactions and consists of three terms as

$$\mathcal{H}_e=\mathcal{H}_J+\mathcal{H}_H+\mathcal{H}_{AF}. \quad (2)$$

$\mathcal{H}_J$ represents the SE interaction between nearest neighboring (NN) e_g electrons derived from the generalized Hubbard model with orbital degeneracy[12] as

$$\mathcal{H}_J=-2J_1\sum_{\langle ij\rangle}\left(\frac{3}{4}n_in_j+\vec{S}_i\cdot\vec{S}_j\right)\left(\frac{1}{4}-\tau_i^l\tau_j^l\right)$$
$$-2J_2\sum_{\langle ij\rangle}\left(\frac{1}{4}n_in_j-\vec{S}_i\cdot\vec{S}_j\right)\left(\frac{3}{4}+\tau_i^l\tau_j^l+\tau_i^l+\tau_j^l\right), \quad (3)$$

where $J_1=t_0^2/(U'-I)$ and $J_2=t_0^2/(U'+I+2J_H)$. U, U', and I are the intra- and interorbital Coulomb interactions, and the exchange interaction for e_g electrons, respectively, and a relation $U=U'+I$ is assumed. J_H is the Hund coupling between e_g electrons and t_{2g} spin $\vec{S}_i^t$ ($S^t=3/2$), and t_0 is the transfer intensity between NN $d_{3z^2-r^2}$ orbitals along the z axis. Energy splitting between two e_g orbitals due to the JT effect is neglected in the denominators of J_1 and J_2, because this splitting is much smaller than the Coulomb interactions.[18,24–33] $\vec{S}_i$ is the spin operator of an e_g electron with $S=1/2$. τ_i^l is defined as $\tau_i^l=\cos(2\pi/3m_l)T_{iz}-\sin(2\pi/3m_l)T_{ix}$ with $(m_x,m_y,m_z)=(1,-1,0)$, where l denotes a direction of a bond connecting sites i and j. $\vec{T}_i$ is the pseudospin operator for the orbital degree of freedom, and $\langle T_{iz}\rangle=+(-)1/2$ corresponds to the state where the $d_{3z^2-r^2}$ ($d_{x^2-y^2}$) orbital is occupied by an electron. The second and third terms in Eq. (2) describe the Hund coupling between e_g and t_{2g} spins and the AF SE interaction (J_{AF}) between NN t_{2g} spins, respectively. These are given by

$$\mathcal{H}_H+\mathcal{H}_{AF}=-J_H\sum_i\vec{S}_i\cdot\vec{S}_i^t+J_{AF}\sum_{\langle ij\rangle}\vec{S}_i^t\cdot\vec{S}_j^t. \quad (4)$$

The second and third terms in Eq. (1) describe the electron-lattice interaction and the lattice dynamics, respectively. Here, we consider the displacement of O ions along the direction connecting NN Mn ions, since the motion of O ions along the other directions does not couple linearly with the e_g orbitals. Thus, $\mathcal{H}_{e\text{-}latt}$ is given by

$$\mathcal{H}_{e\text{-}latt}=-g_{JT}\sum_{il=x,z}Q_{il}T_{il}, \quad (5)$$

where g_{JT} is the coupling constant. Q_{ix} and Q_{iz} are the normal modes of the lattice distortion at site i given by $Q_{ix}=1/\sqrt{2}(-v_{ix}+v_{i-\hat{x}x}+v_{iy}-v_{i-\hat{y}y})$ and $Q_{iz}=1/\sqrt{6}(2v_{iz}-2v_{i-\hat{z}z}-v_{ix}+v_{i-\hat{x}x}-v_{iy}+v_{i-\hat{y}y})$.[16] $v_{i\xi}$ is the displacement of an O ion at $\vec{r}_i+(a/2)\hat{\xi}$ and a is the lattice constant. These normal modes are schematically shown in Fig. 1. The third term in Eq. (1), $\mathcal{H}_{latt}$, is given by

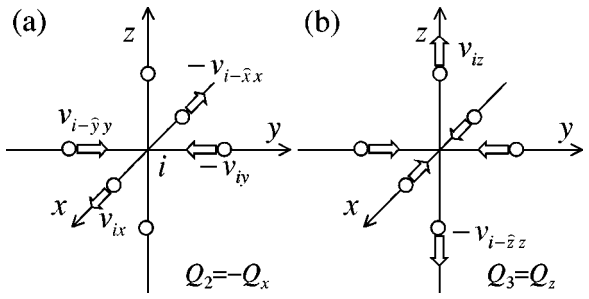

FIG. 1. The modes of the distortion of a MnO_6 octahedron. (a) Q_2 and (b) Q_3 modes.

$$\mathcal{H}_{latt}=\sum_{\vec{k}\xi=x,y,z}\frac{\hbar\omega_{\vec{k}}}{2}(p_{\vec{k}\xi}^*p_{\vec{k}\xi}+q_{\vec{k}\xi}^*q_{\vec{k}\xi}), \quad (6)$$

where $q_{\vec{k}\xi}$ is the normal coordinate of lattice vibration with direction of displacement ξ and momentum $\vec{k}$, and $p_{\vec{k}\xi}$ is the canonical conjugate momentum of $q_{\vec{k}\xi}$. $q_{\vec{k}\xi}$ and $v_{i\xi}$ satisfy the relation $v_{i\xi}=1/\sqrt{N}\Sigma_i e^{i\vec{k}\vec{r}_i}\sqrt{\hbar/m\omega_{\vec{k}}}q_{\vec{k}\xi}$ with N being the total number of Mn sites. The frequency of the lattice vibration is independent of $\vec{k}$ and is given by $\omega_{\vec{k}}=\sqrt{K/m}$ with m being the mass of an O ion, since only the spring constant $K/2$ between NN Mn and O ions is taken into account. $\mathcal{H}_{str}$ and $\mathcal{H}_{e\text{-}str}$ in Eq. (1) describe the elastic energy and electron-strain coupling, respectively,[17] as

$$\mathcal{H}_{str}=\frac{Vc_0}{2}(u_x^2+u_z^2), \quad (7)$$

and

$$\mathcal{H}_{e\text{-}str}=-2g_0\sqrt{\frac{Vc_0}{N}}\sum_i(u_xT_{ix}+u_zT_{iz}). \quad (8)$$

Here V is the volume of the system and c_0 is the elastic constant. The electron-strain coupling constant g_0 is related to g_{JT} as $g_0=a/2\sqrt{N/Vc_0}g_{JT}$. The bulk distortions u_x and u_z are represented by the elastic strain $e_{\rho\rho'}(\rho,\rho'=x,y,z)$ as $u_x=1/\sqrt{2}(e_{yy}-e_{xx})$ and $u_z=1/\sqrt{6}(2e_{zz}-e_{yy}-e_{xx})$, respectively.[17] Schematic pictures of the bulk distortions are presented in Fig. 2. The last term of Eq. (1) describes the higher-order JT coupling given by

$$\mathcal{H}_{hiJT}=-B\frac{Vc_0}{g_0^2N}\sum_i\{(Q_{iz}^2-Q_{ix}^2)T_{iz}-2Q_{iz}Q_{ix}T_{ix}\}, \quad (9)$$

with coupling constant B.

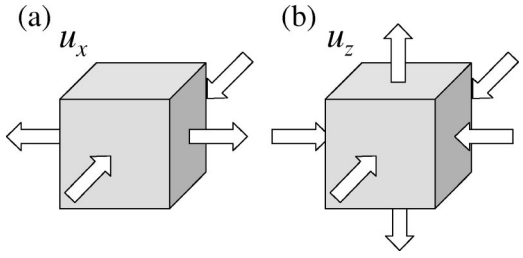

FIG. 2. The modes of the bulk strain. (a) u_x and (b) u_z modes.

Now, we derive the effective Hamiltonian describing the intersite orbital interaction through the exchange of phonons[17] from $\mathcal{H}_{e\text{-}latt}$ and $\mathcal{H}_{latt}$. $\mathcal{H}_{e\text{-}latt}$ is rewritten by using the Fourier transforms of $q_{\vec{k}\xi}=1/\sqrt{N}\Sigma_i e^{-i\vec{k}\vec{r}_i}q_{i\xi}$ and $T_{\vec{k}l}=1/\sqrt{N}\Sigma_i e^{-i\vec{k}\vec{r}_i}T_{il}$ as

$$\mathcal{H}_{e\text{-}latt}=-2\sum_{\substack{\vec{k}l=x,z\\ \xi=x,y,z}}\sqrt{\hbar\omega_{\vec{k}}}g_{\vec{k}\xi l}T_{-\vec{k}l}q_{\vec{k}\xi}. \tag{10}$$

Here, $g_{\vec{k}\xi l}$ is defined as

$$g_{\vec{k}\xi l}=\frac{1}{2}\frac{g_{JT}}{\sqrt{K}}(1-e^{-ik_\xi a})C_{l\xi}, \tag{11}$$

with

$$C_{l\xi}=\begin{pmatrix} \frac{1}{\sqrt{2}} & -\frac{1}{\sqrt{2}} & 0 \\ -\frac{1}{\sqrt{6}} & -\frac{1}{\sqrt{6}} & \frac{2}{\sqrt{6}} \end{pmatrix}_{l\xi}. \tag{12}$$

Then, by using the canonical transformation, the linear couplings between e_g electrons and lattice distortion are eliminated as

$$\mathcal{H}_{e\text{-}latt}+\mathcal{H}_{latt}=-\frac{g_{JT}^2}{K}\sum_{\vec{k}ll'}\tilde{A}_{\vec{k}ll'}T_{-\vec{k}l}T_{\vec{k}l'} +\sum_{i\xi}\frac{\hbar\omega_{\vec{k}}}{2}(\tilde{p}_{\vec{k}\xi}^2+\tilde{q}_{\vec{k}\xi}^2), \tag{13}$$

where

$$\tilde{A}_{\vec{k}ll'}=\frac{1}{2}\begin{pmatrix} 2-c_x-c_y & \frac{1}{\sqrt{3}}(c_x-c_y) \\ \frac{1}{\sqrt{3}}(c_x-c_y) & \frac{1}{3}(6-c_x-c_y-4c_z) \end{pmatrix}_{ll'}, \tag{14}$$

and $c_\rho=\cos k_\rho a$. $\tilde{q}_{\vec{k}\xi}$ is the new phonon coordinate given by

$$\tilde{q}_{\vec{k}\xi}=q_{\vec{k}\xi}-\frac{2}{\sqrt{\hbar\omega_{\vec{k}}}}\sum_l g_{\vec{k}\xi l}^{*}T_{-\vec{k}l}, \tag{15}$$

and $\tilde{p}_{k\xi}$ is the canonical conjugate momentum for $\tilde{q}_{k\xi}$. The first and second terms of the right-hand side in Eq. (13) are denoted by $\tilde{\mathcal{H}}_{o\text{-}o}$ and $\tilde{\mathcal{H}}_{latt}$, respectively. Here, we neglect the noncommutability between $\mathcal{H}$ [Eq. (1)] and $\tilde{q}_{k\xi}$. $\tilde{\mathcal{H}}_{o\text{-}o}$ includes the self-interaction of the orbital, which does not contribute to the orbital order-disorder transition. Therefore, by subtracting this term, we obtain the following form:

$$\mathcal{H}_{o\text{-}o}=-\frac{g_{JT}^2}{K}\sum_{\vec{k}ll'}A_{\vec{k}ll'}T_{-\vec{k}l}T_{\vec{k}l'}, \tag{16}$$

with

$$A_{kll'}=\frac{1}{2}\begin{pmatrix} -c_x-c_y & \frac{1}{\sqrt{3}}(c_x-c_y) \\ \frac{1}{\sqrt{3}}(c_x-c_y) & \frac{1}{3}(-c_x-c_y-4c_z) \end{pmatrix}_{ll'}. \tag{17}$$

Then, we obtain the effective Hamiltonian for the spin, orbital, and lattice degrees of freedom in $LaMnO_3$ given by

$$\mathcal{H}_{eff}=\mathcal{H}_e+\tilde{\mathcal{H}}_{latt}+\mathcal{H}_{o\text{-}o}+\mathcal{H}_{e\text{-}str}+\mathcal{H}_{str}+\mathcal{H}_{hiJT}. \tag{18}$$

III. MEAN-FIELD APPROXIMATION

In order to calculate the orbital ordering temperature from Eq. (18), we introduce the mean-field approximation at finite temperatures. It is experimentally confirmed that the orbital order-disorder transition in $LaMnO_3$ is of the first order but is close to the second-order transition; a discontinuity of the orbital order parameter at T_{OO} is negligible.[5] Therefore, we expect that the higher-order JT coupling, which brings about the first-order phase transition, is much smaller than the linear JT coupling. Thus, we neglect $\mathcal{H}_{hiJT}$ in Eq. (18) and calculate T_{OO}. We will consider $\mathcal{H}_{hiJT}$ in the calculation of the elastic constant presented in Sec. V.

The *A*-type AF spin and *C*-type orbital orderings are observed in $LaMnO_3$.[5–7] Two sublattices for the orbital (spin) ordering are denoted by *A* and *B* (*a* and *b*) and the following mean fields are introduced: $\langle S_{a,bz}\rangle$, $\langle S_{a,bz}^t\rangle$, $\langle T_{A,Bx}\rangle$, and $\langle T_{A,Bz}\rangle$. The free energy of the system is obtained in the mean-field approximation as follows:

$$\begin{aligned}\mathcal{F}_0=&\frac{Vc_0}{2}(u_x^2+u_z^2)-\frac{N}{2}\{6J_{xy}^t\langle T_{Ax}\rangle\langle T_{Bx}\rangle+2J_{xy}^t\langle T_{Az}\rangle\langle T_{Bz}\rangle\\ &+2J_z^t(\langle T_{Az}\rangle^2+\langle T_{Bz}\rangle^2)+J_2(2\langle S_{az}\rangle\langle S_{bz}\rangle-\langle S_{az}\rangle^2\\ &-\langle S_{bz}\rangle^2)(\langle T_{Az}\rangle+\langle T_{Bz}\rangle)\}+\frac{N}{2}(J_1-3J_2)(\langle S_{az}\rangle^2\\ &+\langle S_{bz}\rangle^2+\langle S_{az}\rangle\langle S_{bz}\rangle)-NJ_{AF}(\langle S_{az}^t\rangle^2+\langle S_{az}^t\rangle\langle S_{bz}^t\rangle\\ &+\langle S_{az}^t\rangle^2)-\frac{N}{2\beta}(\ln z_a^s+\ln z_b^s+\ln z_A^t+\ln z_B^t),\end{aligned} \tag{19}$$

where $\beta=1/T$. $z_{a(b)}^s$ and $z_{A(B)}^t$ in the last four terms represent the partition functions of spin and orbital given by $z_{a(b)}^s=\mathrm{Tr}\exp(-\beta\mathcal{H}_{a(b)}^s)$ and $z_{A(B)}^t=\mathrm{Tr}\exp(-\beta\mathcal{H}_{A(B)}^t)$, respectively. $\mathcal{H}_{a(b)}^s$ is the mean-field Hamiltonian describing the spin state in sublattice *a* (*b*) as

$$\mathcal{H}_{a(b)}^s=4J_{xy}^s\langle\tilde{S}_{a(b)z}\rangle\tilde{S}_{a(b)z}+2J_z^s\langle\tilde{S}_{b(a)z}\rangle\tilde{S}_{a(b)z}, \tag{20}$$

where J_{xy}^s and J_z^s represent the effective exchange interaction between NN spins in the *xy* plane and along the *z* direction, respectively. These are explicitly given by

$$J^s_{xy}=-\frac{1}{32}(J_1-3J_2)+\frac{1}{32}(J_1+J_2)(3\langle T_{Ax}\rangle\langle T_{Bx}\rangle+\langle T_{Az}\rangle \times\langle T_{Bz}\rangle)-\frac{1}{16}J_2(\langle T_{Az}\rangle+\langle T_{Bz}\rangle)+\frac{9}{16}J_{AF}, \quad (21)$$

and

$$J^s_z=-\frac{1}{32}(J_1-3J_2)+\frac{1}{8}(J_1+J_2)\langle T_{Az}\rangle^2+\frac{1}{16}J_2(\langle T_{Az}\rangle+\langle T_{Bz}\rangle)+\frac{9}{16}J_{AF}. \quad (22)$$

In Eq. (20), we introduce a spin operator $\tilde{\vec{S}}_i$ with $\tilde{S}=2$, rewrite $\vec{S}_i$ and $\vec{S}^t_i$ as $\vec{S}_i=\frac{1}{4}\tilde{\vec{S}}_i$ and $\vec{S}^t_i=\frac{3}{4}\tilde{\vec{S}}_i$, respectively, and eliminate the largest energy parameter J_H in Eq. (18). Due to the *A*-AF spin structure, the relation $\langle\tilde{S}_{az}\rangle=-\langle\tilde{S}_{bz}\rangle$ is satisfied. $\mathcal{H}^t_{A(B)}$ is the mean-field Hamiltonian describing the orbital state in sublattice *A* (*B*) as

$$\mathcal{H}^t_{A(B)}=6J^t_{xy}\langle T_{B(A)x}\rangle T_{A(B)x}+2\tilde{J}T_{A(B)z}+(2J^t_{xy}\langle T_{B(A)z}\rangle+4J^t_z\langle T_{A(B)z}\rangle)T_{A(B)z}-2g_0\sqrt{\frac{Vc_0}{N}}(u_xT_{A(B)x}+u_zT_{A(B)z}), \quad (23)$$

where $J^t_{xy(z)}$ and $\tilde{J}$ are

$$J^t_{xy(z)}=\frac{1}{4}(3J_1-J_2)+(J_1+J_2)\langle S_{iz}\rangle\langle S_{i+\hat{x}(i+\hat{z})z}\rangle \quad (24)$$

and

$$\tilde{J}=2J_2(\langle S_{az}\rangle^2-\langle S_{az}\rangle\langle S_{bz}\rangle), \quad (25)$$

respectively. For the observed *C*-type orbital ordered state, we have the following conditions: $\langle T_{Az}\rangle=\langle T_{Bz}\rangle$ and $\langle T_{Ax}\rangle=-\langle T_{Bx}\rangle$.

By minimizing the free energy $\mathcal{F}_0$ with respect to $\langle T_{Al}\rangle$ for $l=x,z$ and $\langle\tilde{S}_{az}\rangle$, the following self-consistent equations are obtained:

$$\langle T_{Al}\rangle=\mathrm{Tr}\{T_{Al}\exp(-\beta\mathcal{H}^t_A)\}/z^t_A, \quad (26)$$

$$\langle\tilde{S}_{az}\rangle=\mathrm{Tr}\{\tilde{S}_{az}\exp(-\beta\mathcal{H}^s_a)\}/z^s_a. \quad (27)$$

Equations (26) and (27) are numerically solved under the conditions of $u_z=2g_0\sqrt{N/Vc_0}\langle T_{Az}\rangle$ and $u_x=0$ which are derived from $\partial\mathcal{F}/\partial u_x=0$ and $\partial\mathcal{F}/\partial u_x=0$, respectively.

IV. TRANSITION TEMPERATURES AND SPIN-WAVE DISPERSION

Among several parameters in the Hamiltonian Eqs. (1) and (18), values of J_1,J_2 and g_{JT} are determined by calculating the spin and orbital ordering temperatures and the spin-wave dispersion relation. The other parameters are chosen to be $J_{AF}=1$, $a^2K=17\times10^4$, and $a^3c_0=2\times10^4$ meV, which are derived from the Néel temperature in $CaMnO_3$,[6] the phonon frequency determined by the infrared-absorption spectra[36] and the elastic constant.[37] The lattice constant *a* and the static JT distortion $Q(=\sqrt{Q^2_{iz}+Q^2_{ix}})$ are chosen to be $a=4$ Å and $Q=0.3$ Å, respectively.[38]

First, we calculate the transition temperatures. The orbital ordering temperature in the mean-field approximation T^{MF}_{OO} is given by

$$T^{MF}_{OO}=\frac{1}{2}\left\{\frac{3}{4}(3J_1-J_2)+\frac{g^2_{JT}}{K}\right\}, \quad (28)$$

and the Néel temperature for the *A*-AF ordering T^{MF}_N is given by the solution of the following equation:

$$T^{MF}_N=-8J^s_{xy}+4J^s_z, \quad (29)$$

where J^s_{xy} and J^s_z defined in Eqs. (21) and (22) are the functions of T^{MF}_N. By fitting T^{MF}_{OO} and T^{MF}_N to the experimental transition temperatures $T_{OO}=780$ K (Ref. 5) and $T_N=140$ K (Refs. 6 and 7), respectively, J_2 and $g_{JT}Q$ are calculated as functions of J_1. In general, the mean-field approximation tends to overestimate the transition temperature. Therefore, we also estimate the parameter values of J_1, J_2, and $g_{JT}Q$ by considering the correction of the mean-field transition temperatures. For the Néel temperature, we revise T^{MF}_N as bT^{MF}_N with $b=0.63$, which is the ratio between T_N for the $S=1/2$ AF Heisenberg model obtained in the high-temperature expansion and that in the mean-field approximation.[39] As for the orbital ordering temperature, we revise as aT^{MF}_{OO} with $a=0.75$, which is obtained by the calculation of T_N for the $S=1/2$ AF Ising model.[39] This is because the orbital part of the Hamiltonian [Eq. (3)] has a discontinuous symmetry, although this symmetry is higher than that of the Ising model.

The spin stiffness constant provides another condition for J_1,J_2 and g_{JT}. Although the JT distortion does not directly couple with the spin degree of freedom, g_{JT} modifies the orbital state and affects the SE interaction between NN spins. We calculate the spin-wave dispersion at $T=0$ and compare it with the experimental one. Here, the orbital and lattice degrees of freedom are assumed to be frozen, since the energy scale of orbital excitations[12,40] and optical phonons are much larger than that of spin waves. Then, the relevant parts of the Hamiltonian in Eq. (1) are given by

$$\mathcal{H}_{SW}=\mathcal{H}_e+\mathcal{H}_{e\text{-}latt}. \quad (30)$$

The static distortion of a MnO_6 octahedron is written as $(Q_{iz},Q_{ix})=Q(\cos\theta^{JT}_i,\sin\theta^{JT}_i)$ where $\theta^{JT}_A=-\theta^{JT}_B=2\pi/3$. The orbital ordered state is determined in the mean-field approximation.[34] By applying the Holstein-Primakoff transformation to the spin operators, the dispersion relation of the spin wave is calculated. Experimentally, the spin wave in $LaMnO_3$ was measured by the neutron-scattering experiments in Refs. 11 and 35. The authors in these papers analyzed the experimental data by using the Heisenberg model with the NN SE interactions. They obtained the magnitude of the interaction in the *xy* plane (J^s_{xy}) and that in the *z* axis (J^s_z), which are defined in Eqs. (21) and (22) as $2J^s_{xy}=-3.34$ meV and $2J^s_z=2.42$ meV.

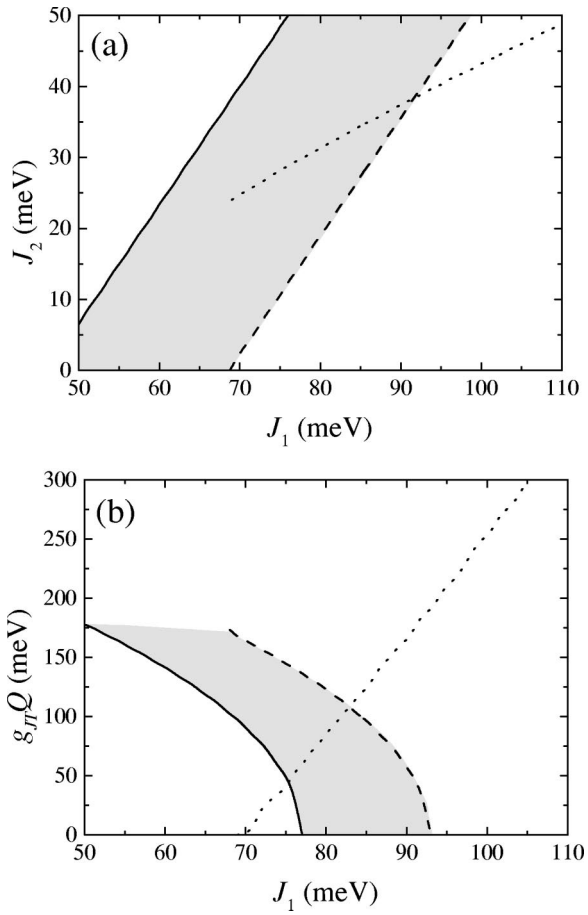

FIG. 3. (a) J_2 and (b) $g_{JT}Q$ as functions of J_1. Solid and broken curves are obtained from the analyses of transition temperatures T_{OO} and T_N. For broken curves, the correction from the mean-field approximation is taken into account (see the text). The actual values of the parameters are expected to exist in the shaded regions. Dotted curves are obtained from the analysis of the spin stiffness constants. Other parameter values are chosen to be $J_{AF}=1$ meV, $a^2K=17\times10^4$ meV, $B=0$ meV, $Q=0.3$ Å, and $a=4$ Å.

By fitting the theoretical results of the orbital ordering temperature, the Néel temperature for the *A*-AF ordering, and the spin stiffness constant to the experimental values, we estimate J_1, J_2, and g_{JT}. J_2 and $g_{JT}Q$ are plotted as functions of J_1 in Figs. 3(a) and 3(b), respectively. Solid and broken curves are obtained from the transition temperatures, T_{OO} and T_N. The actual values of the parameters are expected to exist in the shaded regions. Dotted curves are obtained from the spin stiffness constants. The analyses for T_{OO} and T_N [solid and broken curves in Figs. 3(a) and 3(b)] show that J_2 increases and $g_{JT}Q$ decreases with increasing J_1. This is because $(3J_1-J_2)$ and g_{JT}^2/K contribute cooperatively to T_{OO}, as shown in Eq. (28). On the other hand, the analyses for the spin stiffness constant [dotted curves in Figs. 3(a) and 3(b)] show that both J_2 and $g_{JT}Q$ increase with increasing J_1, i.e., J_1 competes with both J_2 and $g_{JT}Q$. This is attributed to the facts that (i) J_1 and J_2 are the ferromagnetic and antiferromagnetic interactions, respectively, and (ii) $g_{JT}Q$ favors the $(d_{3x^2-r^2}/d_{3y^2-r^2})$-type orbital ordered state where the ferromagnetic interaction in the xy plane caused by J_1 is weaker than that without $g_{JT}Q$. The magnitudes of J_1, J_2, and $g_{JT}Q$ are obtained from the intersection points of solid (broken) curves and dotted curves in Figs. 3(a) and 3(b). We obtain $J_1=75$–85 meV, $J_2=25$–40 meV, and $E_{JT}=g_{JT}Q=50$–100 meV. It is stressed that the value of E_{JT} is much smaller than that in the literature, i.e., $E_{JT}>1$ eV.[18,24–32] In the case that $a^2K=17\times10^4$ meV, the coupling constant of the intersite orbital interaction through the exchange of phonons g_{JT}^2/K is about 3–10 meV which is much smaller than J_1. We conclude that the small E_{JT} comes from the strong Coulomb interaction and the orbital ordering in $LaMnO_3$ is dominated by the interaction through the virtual exchange of electrons. If J_1 and J_2 are neglected to estimate T_{OO}, we obtain E_{JT} to be 400–700 meV for $a^2K=17\times10^4$ meV (Ref. 35) and 600–1100 meV for $a^2K=40\times10^4$ meV.[18] The latter value of E_{JT} is of the same order of magnitude given in Ref. 18.

V. ELASTIC CONSTANTS

The elastic constants provide information of the higher-order JT coupling,[17,19] although the coupling constant B is supposed to be smaller than that in the linear JT coupling. In this section, we examine the elastic constants taking into account the electron-electron and electron-lattice interactions, and the higher-order JT coupling.

We start with the model Hamiltonian in Eq. (18). The elastic constants are the coefficients of the δu_l^2 terms in the free energy, where δu_l is the deviation of strain u_l from that in the thermal equilibrium. Here, the deviations of T_{Al} and T_{Bl} from the thermal equilibriums, δT_{Al} and δT_{Bl}, are also introduced. δT_{Al} and δT_{Bl} are induced by an external strain $\delta u_{l'}$ and the relations between them are derived later. Now, the free energy is expanded up to the second order of δT_{Al}, δT_{Bl}, and δu_l as

$$\mathcal{F}=\tilde{\mathcal{F}}_0+\frac{Vc_0}{2}(\delta u_x^2+\delta u_z^2)-\frac{N}{2}[6J_{xy}^t\delta T_{Ax}\delta T_{Bx}+2J_{xy}^t\delta T_{Az}\delta T_{Bz}+2J_z^t\{(\delta T_{Az}+\delta T_{Bz})^2-(\delta T_{Az}-\delta T_{Bz})^2\}]-\frac{\beta N}{4}\{F_{xx}(C_x^{A2}+C_x^{B2})+F_{zz}(C_x^{A2}+C_x^{B2})+2F_{xz}(C_x^AC_z^A-C_x^BC_z^B)\}. \quad (31)$$

Here, $\tilde{\mathcal{F}}_0$ is given by Eq. (19) where $z_{A(B)}^t$ is replaced by $z_{A(B)}^t=\mathrm{Tr}\exp(-\beta\tilde{\mathcal{H}}_{A(B)}^t)$, with $\tilde{\mathcal{H}}_{A(B)}^t$ being given by

$$\tilde{\mathcal{H}}_{A(B)}^t=\mathcal{H}_{A(B)}^t-B\frac{Vc_0}{Ng_0}\{(Q_{A(B)z}^2-Q_{A(B)x}^2)T_{A(B)z}-2Q_{A(B)z}Q_{A(B)x}T_{A(B)x}\}. \quad (32)$$

The last term of this equation comes from the higher-order JT coupling. We assume that the equilibrium values of Q_{Al} appearing in this term are given by $Q_{Az}=au_z$ and $Q_{Ax}=4(g_{JT}/K)\langle T_{Ax}\rangle$ by considering the definition of the strain u_z and the linear JT coupling in Eq. (5). C_l^α's are the coefficients of $T_{\alpha l}$ except for $\tilde{J}$ in $\mathcal{H}_\alpha^t$ [Eq. (23)] where $\langle T_{Al}\rangle$,

$\langle T_{Bl}\rangle$, and u_l are replaced by δT_{Al}, δT_{Bl}, and δu_l, respectively. Their explicit forms are given by

$$C_x^A = 6J_{xy}^t \delta T_{Bx} - 2g_0 \sqrt{\frac{Vc_0}{N}} \delta u_x, \tag{33}$$

$$C_z^A = 2J_{xy}^t \delta T_{Bz} + 4J_z^t \delta T_{Az} - 2g_0 \sqrt{\frac{Vc_0}{N}} \delta u_z, \tag{34}$$

$$C_x^B = 6J_{xy}^t \delta T_{Ax} - 2g_0 \sqrt{\frac{Vc_0}{N}} \delta u_x, \tag{35}$$

$$C_z^B = 2J_{xy}^t \delta T_{Az} + 4J_z^t \delta T_{Bz} - 2g_0 \sqrt{\frac{Vc_0}{N}} \delta u_z. \tag{36}$$

Here, the term originating from the higher-order JT coupling is neglected.[17] $F_{ll'}$ in Eq. (31) represents the self-correlation function of the orbital given by

$$F_{ll'} = \langle T_{Al}\rangle\langle T_{Al'}\rangle - K_{ll'} \tag{37}$$

with

$$K_{ll'} = \frac{1}{z_A^t}\left[\sum_{mm'} e^{-\beta\varepsilon_m}\delta_{\varepsilon_m,\varepsilon_{m'}} - \frac{2}{\beta}\sum_{\substack{m>m' \\ (\varepsilon_m\neq\varepsilon_{m'})}} \frac{e^{-\beta\varepsilon_m} - e^{-\beta\varepsilon_{m'}}}{\varepsilon_m - \varepsilon_{m'}}\right] \times (T_{Al})_{mm'}(T_{Al'})_{m'm}, \tag{38}$$

where ε_m represents the mth eigenvalue of $\tilde{\mathcal{H}}_A^t$. To derive Eq. (31), the conditions $\langle T_{Ax}\rangle = -\langle T_{Bx}\rangle$, $\langle T_{Az}\rangle = \langle T_{Bz}\rangle$, $Q_{Az} = Q_{Bz}$, and $Q_{Ax} = -Q_{Bx}$ are used. By using the condition $\partial\mathcal{F}/\partial\delta T_{\alpha l} = 0$, the following relations between δu_l's and $\delta T_{\alpha l'}$'s are obtained:

$$\delta T_{Ax} + \delta T_{Bx} = -\frac{4\beta g_0}{D_x}\sqrt{\frac{Vc_0}{N}}\delta u_x \times [F_{xx}\{1-(4J_z^t - 2J_{xy}^t)\beta F_{zz}\} + (4J_z^t - 2J_{xy}^t)\beta F_{xz}^2], \tag{39}$$

$$\delta T_{Az} - \delta T_{Bz} = -\frac{4\beta g_0}{D_x}\sqrt{\frac{Vc_0}{N}}\delta u_x F_{xz}, \tag{40}$$

$$\delta T_{Az} + \delta T_{Bz} = -\frac{4\beta g_0}{D_z}\sqrt{\frac{Vc_0}{N}}\delta u_z \times \{F_{zz}(1-6J_{xy}^t\beta F_{xx}) + 6J_{xy}^t\beta F_{xz}^2\}, \tag{41}$$

$$\delta T_{Ax} - \delta T_{Bx} = -\frac{4\beta g_0}{D_z}\sqrt{\frac{Vc_0}{N}}\delta u_z F_{xz}, \tag{42}$$

with

$$D_x = (1-6J_{xy}^t\beta F_{xx})\{1-(4J_z^t - 2J_{xy}^t)\beta F_{zz}\} - 6J_{xy}^t(4J_z^t - 2J_{xy}^t)\beta^2 F_{xz}^2, \tag{43}$$

and

$$D_z = (1+6J_{xy}^t\beta F_{xx})\{1-(4J_z^t + 2J_{xy}^t)\beta F_{zz}\} + 6J_{xy}^t(4J_z^t + 2J_{xy}^t)\beta^2 F_{xz}^2. \tag{44}$$

By using Eqs. (39)–(42), the deviation of the free energy from the equilibrium value is given by

$$\mathcal{F} - \tilde{\mathcal{F}}_0 = \frac{1}{2}[c_x(T)\,\delta u_x^2 + c_z(T)\,\delta u_z^2]. \tag{45}$$

Note that the term proportional to $\delta u_x \delta u_z$ is absent because of the tetragonal symmetry. $c_x(T)$ and $c_z(T)$ are the temperature-dependent elastic constants for the u_x and u_z modes, respectively. Their explicit forms are given by

$$c_x(T) = \frac{c_0}{D_x}[\{1-(6J_{xy}^t - 4g_0^2)\beta F_{xx}\}\{1-(4J_z^t - 2J_{xy}^t)\beta F_{zz}\} - (6J_{xy}^t - 4g_0^2)(4J_z^t - 2J_{xy}^t)\beta^2 F_{xz}^2], \tag{46}$$

and

$$c_z(T) = \frac{c_0}{D_z}[(1+6J_{xy}^t\beta F_{xx})\{1-(4J_z^t + 2J_{xy}^t - 4g_0^2)\beta F_{zz}\} + 6J_{xy}^t(4J_z^t + 2J_{xy}^t - 4g_0^2)\beta^2 F_{xz}^2]. \tag{47}$$

For $T > T_{OO}$, $c_x(T)$ and $c_z(T)$ are simplified as

$$c_x(T) = c_z(T) = c_0\frac{T + \frac{3}{8}(3J_1 - J_2) + \frac{1}{2}\frac{g_{JT}^2}{K} - g_0^2}{T + \frac{3}{8}(3J_1 - J_2) + \frac{1}{2}\frac{g_{JT}^2}{K}}. \tag{48}$$

The elastic constants are numerically calculated and presented as functions of T in Fig. 4. Parameter values are chosen to be $J_1 = 75$ meV, $J_2 = 25$ meV, $J_{AF} = 1$ meV, $ag_{JT} = 6\times10^2$ meV, $a^2K = 17\times10^4$ meV, and $a^3c_0 = 2\times10^4$ meV. The higher-order JT coupling B is chosen to be $B = 0$ meV in Fig. 4(a) and $B = 50$ meV in Fig. 4(b). When B is comparable to J_1, the discontinuous change in the elastic constants is found at T_{OO}. We also obtain a change in c_x at T_N. This change reflects the change of the orbital state. As shown in Fig. 5, when B is much smaller than J_1 (solid curve), the orbital ordered state of the $1/\sqrt{2}(d_{3z^2-r^2} + d_{x^2-y^2}/d_{3z^2-r^2} - d_{x^2-y^2})$-type above T_N changes to the state below T_N where the component of the $(d_{y^2-z^2}/d_{z^2-x^2})$-type increases. On the other hand, when B is comparable to J_1 (broken curve), the component of the $1/\sqrt{2}(d_{3z^2-r^2} + d_{x^2-y^2}/d_{3z^2-r^2} - d_{x^2-y^2})$-type state increases below T_N. These changes of the orbital states originate from the spin-orbital coupling in $\mathcal{H}_J$ in Eq. (3). The changes of the elastic constants are understood as follows: In the $1/\sqrt{2}(d_{3z^2-r^2} + d_{x^2-y^2}/d_{3z^2-r^2} - d_{x^2-y^2})$-type orbital ordered state, $\langle T_{Ax}\rangle$ is almost saturated as $|\langle T_{Ax}\rangle| = 1/2$ and $\langle T_{Az}\rangle = 0$. Thus, the external strain δu_x does not induce δT_{Ax}, and c_x is saturated. The deviation of the orbital state from the $1/\sqrt{2}(d_{3z^2-r^2} + d_{x^2-y^2}/d_{3z^2-r^2} - d_{x^2-y^2})$-type one causes the decrease of c_x as shown in Fig. 4. This fact reminds us of the inverse of the parallel spin susceptibility $1/\chi_{\parallel}$

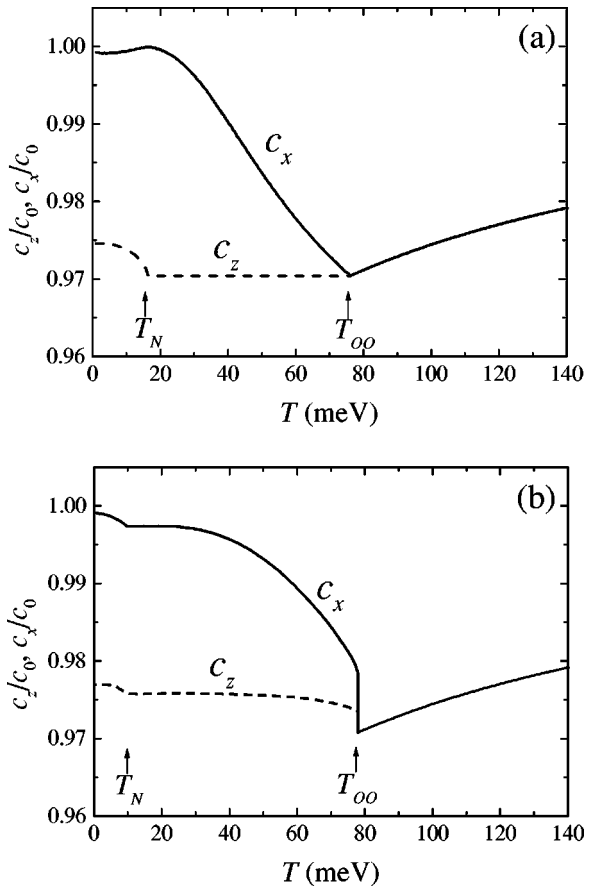

FIG. 4. The elastic constants as functions of T. Solid and broken curves denote c_x and c_z, respectively. Parameter values are chosen to be $J_1=75$ meV, $J_2=25$ meV, $J_{AF}=1$ meV, $ag_{JT}=6\times10^2$ meV, $a^2K=17\times10^4$ meV, and $a^3c_0=2\times10^4$ meV. The value of B is chosen as $B=0$ meV in (a) and $B=50$ meV in (b).

diverging with decreasing T in an antiferromagnet. We propose that the characteristic change of the elastic constant at T_N may be used to estimate the coupling constant B.

VI. SUMMARY AND DISCUSSION

We have examined the orbital ordering in $LaMnO_3$ and the magnitudes of the interactions of the e_g orbitals between NN sites caused by the virtual exchange of electrons and phonons. By calculating the orbital and spin ordering temperatures, and the spin-wave dispersion and comparing them with the experimental results, we obtained $J_1=75-85$ meV, $J_2=25-40$ meV, and $g_{JT}Q=E_{JT}=50-100$ meV. E_{JT} is much smaller than that in the literature[18,24–32] which were estimated by neglecting the electron-electron interaction. The present results indicate that the orbital ordering in $LaMnO_3$ is mainly caused by virtual exchange of electrons under the strong Coulomb interactions.[21,22] We calculate the temperature dependence of the elastic constants by taking into account both the electron-electron and electron-lattice interactions. It is predicted that the elastic constants show the characteristic change at T_N which depends on the magnitude of the higher-order JT coupling; when the coupling constant B is comparable to J_1 (much smaller than J_1), c_x increases (decreases) with decreasing T. Through the detailed comparison between theory and experiment, the value of B may be determined.

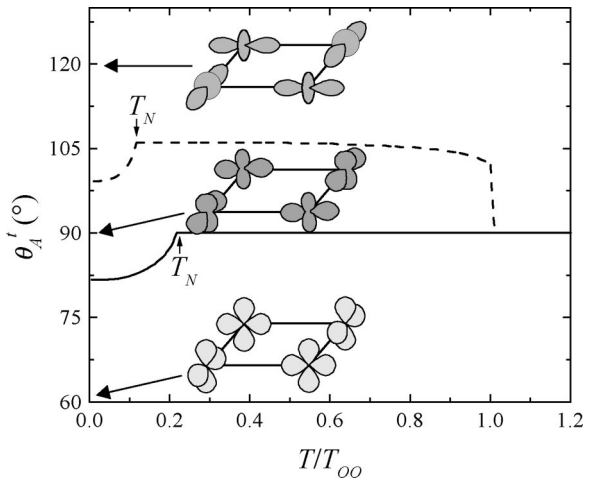

FIG. 5. Temperature dependence of the orbital state. θ_A^t is defined by $\theta_A^t=\tan^{-1}(\langle T_{Ax}\rangle/\langle T_{Az}\rangle)$. Solid and broken curves are the results for $B=0$ meV and $B=50$ meV, respectively. Other parameter values are the same as those in Fig. 4. The insets show the schematic orbital structures in the xy plane.

The present results support the recent report on the observation of the collective orbital excitation termed orbital wave in $LaMnO_3$ by the Raman-scattering experiments. Saitoh *et al.* have observed three peak structures around 120–160 meV in the Raman spectra.[40] These peaks can be explained by neither the two-phonon excitations nor the magnetic excitations. The theoretical results of the Raman spectra from the orbital wave agree with the polarization dependence of the spectra and their relative intensities in experiment.[41] Since the characteristic energy of the orbital excitation is much higher than that of the lattice vibration, we introduce the adiabatic approximation for the lattice degree of freedom in the calculation of the orbital wave. Then, the energy of orbital wave is approximately given by $\omega_{orb}=\sqrt{(3J_1+\sqrt{3}/2E_{JT})(J_1+J_2+\sqrt{3}/2E_{JT})}$. When we adopt the parameter values obtained in the present analyses $J_1=75$ meV, $J_2=25$ meV, and $E_{JT}=50$ meV, we obtain $\omega_{orb}=196$ meV. These numerical values are consistent with the observed energies of the Raman shifts from the orbital excitations.

ACKNOWLEDGMENTS

The authors would like to thank T. A. Kaplan, T. Goto, H. Hazama, N. Nagaosa, Y. Tokura, and E. Saitoh for their valuable discussions. This work was supported by a Grant-in-Aid for Scientific Research Priority Area from the Ministry of Education, Science, Sports, Culture, and Technology of Japan, CREST Japan and Science and Technology Special Coordination Fund for Promoting Science and Technology. Part of the numerical calculation was performed in the supercomputing facilities in the Institute for Materials Research, Tohoku University. S.M. acknowledges support of the Humboldt Foundation.

[1] Y. Tokura and N. Nagaosa, Science **288**, 462 (2000).
[2] K. Chahara, T. Ohno, M. Kasai, Y. Kanke, and Y. Kozono, Appl. Phys. Lett. **62**, 780 (1993).
[3] R. von Helmolt, J. Wecker, B. Holzapfel, L. Schultz, and K. Samwer, Phys. Rev. Lett. **71**, 2331 (1993).
[4] Y. Tokura, A. Urushibara, Y. Moritomo, T. Arima, A. Asamitsu, G. Kido, and N. Furukawa, J. Phys. Soc. Jpn. **63**, 3931 (1994).
[5] Y. Murakami, J. P. Hill, D. Gibbs, M. Blume, I. Koyama, M. Tanaka, H. Kawata, T. Arima, Y. Tokura, K. Hirota, and Y. Endoh, Phys. Rev. Lett. **81**, 582 (1998).
[6] E. O. Wollan and W. C. Koehler, Phys. Rev. **100**, 545 (1955).
[7] G. Matsumoto, J. Phys. Soc. Jpn. **29**, 606 (1970).
[8] J. B. Goodenough, Phys. Rev. **100**, 564 (1955); in *Progress in Solid State Chemistry*, edited by H. Reiss (Pergamon, London, 1971), Vol. 5.
[9] J. Kanamori, J. Phys. Chem. Solids **10**, 87 (1959).
[10] K. I. Kugel and D. I. Khomskii, Zh. Éksp. Teor. Fiz. **64**, 1429 (1973) [Sov. Phys. JETP **37**, 725 (1973)].
[11] K. Hirota, N. Kaneko, A. Nishizawa, and Y. Endoh, J. Phys. Soc. Jpn. **65**, 3736 (1996).
[12] S. Ishihara, J. Inoue, and S. Maekawa, Physica C **263**, 130 (1996); Phys. Rev. B **55**, 8280 (1997).
[13] J. Rodriguez-Carvajal, M. Hennion, F. Moussa, A. H. Moudden, L. Pinsard, and A. Revcolevschi, Phys. Rev. B **57**, R3189 (1998).
[14] R. Maezono, S. Ishihara, and N. Nagaosa, Phys. Rev. B **57**, R13 993 (1998).
[15] D. Feinberg, P. Germain, M. Grilli, and G. Seibold, Phys. Rev. B **57**, R5583 (1998).
[16] J. Kanamori, J. Appl. Phys. **31**, 14S (1960).
[17] M. Kataoka and J. Kanamori, J. Phys. Soc. Jpn. **32**, 113 (1972).
[18] A. J. Millis, Phys. Rev. B **53**, 8434 (1996).
[19] M. Kataoka, J. Phys. Soc. Jpn. **70**, 2353 (2001).
[20] N. Nagaosa, S. Murakami, and H. C. Lee, Phys. Rev. B **57**, R6767 (1998).
[21] L. F. Feiner and A. M. Oleś, Phys. Rev. B **59**, 3295 (1999).
[22] P. Benedetti and R. Zeyher, Phys. Rev. B **59**, 9923 (1999).
[23] J. Baľa and A. M. Oleś, Phys. Rev. B **62**, R6085 (2000).
[24] J. H. Jung, K. H. Kim, T. W. Noh, E. J. Choi, and Jaejun Yu, Phys. Rev. B **57**, R11 043 (1998).
[25] A. Machida, Y. Moritomo, and A. Nakamura, Phys. Rev. B **58**, 12 540 (1998).
[26] M. Quijada, J. Černe, J. R. Simpson, H. D. Drew, K. H. Ahn, A. J. Millis, R. Shreekala, R. Ramesh, M. Rajeswari, and T. Venkatesan, Phys. Rev. B **58**, 16 093 (1998).
[27] P. B. Allen and V. Perebeinos, Phys. Rev. Lett. **83**, 4828 (1999).
[28] J. M. Coey, M. Viret, and S. von Molnár, Adv. Phys. **48**, 167 (1999).
[29] K. H. Ahn and A. J. Millis, Phys. Rev. B **61**, 13 545 (2000).
[30] S. Satpathy, Z. S. Popović, and F. R. Vukajlović, J. Appl. Phys. **79**, 4555 (1996).
[31] Z. Popovic and S. Satpathy, Phys. Rev. Lett. **84**, 1603 (2000).
[32] L. Hozoi, A. H. de Vries, and R. Broer, Phys. Rev. B **64**, 165104 (2001).
[33] T. Saitoh, A. E. Bocquet, T. Mizokawa, H. Namatame, A. Fujimori, M. Abbate, Y. Takeda, and M. Takano, Phys. Rev. B **51**, 13 942 (1995).
[34] S. Okamoto, S. Ishihara, and S. Maekawa, Phys. Rev. B **61**, 451 (2000); *ibid.* **61**, 14 647 (2000).
[35] F. Moussa, M. Hennion, J. Rodriguez-Carvajal, H. Moudden, L. Pinsard, and A. Revcolevschi, Phys. Rev. B **54**, 15 149 (1996).
[36] T. Arima, Y. Tokura, and J. B. Torrance, Phys. Rev. B **48**, 17 006 (1993); T. Arima and Y. Tokura, J. Phys. Soc. Jpn. **64**, 2488 (1995).
[37] H. Hazama, T. Goto, Y. Nemoto, Y. Tomioka, A. Asamitsu, and Y. Tokura, Phys. Rev. B **62**, 15 012 (2000).
[38] J. F. Mitchell, D. N. Argyriou, C. D. Potter, D. G. Hinks, J. D. Jorgensen, and S. D. Bader, Phys. Rev. B **54**, 6172 (1996).
[39] D. C. Jou and H. H. Chen, Phys. Lett. **45A**, 239 (1973).
[40] E. Saitoh, S. Okamoto, K. Takahashi, K. Tobe, K. Yamamoto, T. Kimura, S. Ishihara, S. Maekawa, and Y. Tokura, Nature (London) **410**, 180 (2001).
[41] S. Okamoto, S. Ishihara, and S. Maekawa, cond-mat/0108032 (unpublished).